Substitutional carbon in $Si_{1-x}Ge_x$

L. Hoffmann, B. Bech Nielsen, and A. Nylandsted Larsen
Institute of Physics and Astronomy, Aarhus University, DK-8000 Aarhus C, Denmark

P. Leary and R. Jones
Department of Physics, University of Exeter, EX44QL Exeter, United Kingdom

P. R. Briddon
Department of Physics, University of Newcastle upon Tyne, Newcastle upon Tyne, NE1 7RU, United Kingdom

S. Öberg
Department of Mathematics, University of Luleå, S-95 187, Luleå, Sweden

(Received 16 February 1999; revised manuscript received 22 June 1999)

Local vibrational modes of carbon impurities in relaxed $Si_{1-x}Ge_x$ have been studied with infrared absorption spectroscopy in the composition range $0.05 \leqslant x \leqslant 0.50$. Carbon modes with frequencies in the range 512–600 cm^{-1} are observed in $^{13}C^+$-implanted $Si_{1-x}Ge_x$ after annealing at 550 °C. Measurements on samples coimplanted with $^{12}C^+$ and $^{13}C^+$ show that these modes originate from defects containing a single carbon atom and from the variation of the mode frequencies with composition *x*, the modes are assigned to substitutional carbon in $Si_{1-x}Ge_x$. Based on the frequencies obtained from a simple vibrational model, the observed modes are assigned to specific combinations of the four Si and Ge neighbors to the carbon. The intensities of the modes indicate that the combination of the four neighbors deviates from a random distribution. *Ab initio* local-density-functional cluster theory has been applied to calculate the structure and the local mode frequencies of substitutional carbon with *n* Ge and $4-n$ Si neighbors in a Si and a Ge cluster. The calculated frequencies are ~9% higher than those observed, but the ordering and the splitting of the mode frequencies agree with our assignments. [S0163-1829(99)01243-6]

I. INTRODUCTION

Layers of $Si_{1-x}Ge_x$ grown on Si substrates have been studied extensively due to the potential applications of band-gap engineering and production of ultrafast electronic devices.[1] A basic limitation arises from the 4% mismatch between the Si and Ge lattice constants, which results in formation of strain-relieving misfit dislocations, when the layer thickness exceeds a critical value, e.g., ~200 Å in $Si_{0.80}Ge_{0.20}$ (Ref. 2). The strain in a $Si_{1-x}Ge_x$ layer can be compensated, if C atoms are added to the alloy.[3] High-quality $Si_{1-x-y}Ge_xC_y$ layers, several hundred nanometers thick, have been obtained by nonequilibrium techniques, such as molecular-beam epitaxy (MBE),[4,5] combined ion and molecular-beam deposition,[6] chemical vapor deposition,[7–8] and ion implantation followed by solid-phase regrowth.[9] In these alloys, most of the C atoms are believed to be located at substitutional sites.[3–9] Below, we use the label C_s for substitutional C. Detailed knowledge about the physical properties of C_s in $Si_{1-x}Ge_x$ may elucidate important aspects of the $Si_{1-x-y}Ge_xC_y$ alloy formation. Moreover, C atoms are common impurities in $Si_{1-x}Ge_x$ compounds. Therefore, C_s in $Si_{1-x}Ge_x$ is an interesting defect. We expect that for C_s, the C atom forms covalent bonds with its four neighbor atoms but the preferential composition of Si and Ge neighbors is unknown. In pure Si and Ge, C_s has a single three-dimensional local mode (T_2) with frequency at 607 and 531 cm^{-1}, respectively.[10,11] This demonstrates that the frequencies associated with stretching of Si-C and Ge-C bonds are well separated. Hence, the frequencies of the C_s modes in $Si_{1-x}Ge_x$ may distinguish the different combinations of Si and Ge neighbors. So far, only the Si-C mode at 607 cm^{-1} has been observed in $Si_{1-x-y}Ge_xC_y$ alloys and it remains unknown whether Ge-C bonds are formed.[3,5,6,8,9]

The present paper addresses this problem. Strain-relaxed $Si_{1-x}Ge_x$ samples implanted with C ions have been investigated by infrared absorption spectroscopy. Strong evidence is presented that C_s in $Si_{1-x}Ge_x$ may bond to Si as well as Ge neighbors and several different neighbor combinations are identified.

A short report on preliminary results of this paper has been published previously by our group.[12] Resently, Kulik *et al.* also reported on the vibrational properties of C_s in SiGe alloys.[13] The sample production and the theoretical analysis applied by these authors differ from the methods used in this paper.

II. EXPERIMENTAL DETAILS

Relaxed, epitaxial $Si_{1-x}Ge_x$ layers with compositions $x = 0.05$, 0.15, 0.25, 0.35, and 0.50 were grown on Si substrates by MBE. Samples with $x > 0.50$ were not studied due to the unsatisfactory crystalline quality obtained in this composition range. The growth technique and the characterization of the $Si_{1-x}Ge_x$ layers were described previously,[14,15] and only a brief account is given here. First, a 1-μm Si layer was grown on a high-resistivity, float-zone, single-crystalline, ⟨100⟩ Si wafer. On top of this layer, a graded SiGe buffer layer was grown with a grading rate of 10 at. % Ge/μm. Finally, a 4 μm-thick $Si_{1-x}Ge_x$ top layer of uniform

composition x was grown. Transmission electron microscopy, photoluminescence, atomic force microscopy, and ion channeling measurements confirmed the high-crystalline quality of the $Si_{1-x}Ge_x$ top layer.[14,15] Samples with typical dimensions of $\sim 8\times 8\times 0.5\,mm^3$ were cut from the wafers, and the $8\times 8\,mm^2$ backside surface of the Si substrate was mechanically polished to ensure large transmission of infrared light.

In most cases, the $Si_{1-x}Ge_x$ layers were implanted with $^{13}C^+$ ions. For the ^{12}C isotope, the relevant infrared absorption lines fall in the same frequency band as the most dominant multiphonon absorption from the Si substrate. For the ^{13}C isotope, the corresponding lines fall at lower frequencies, where the background absorption is reduced significantly. Therefore, the ^{13}C isotope has been applied in this paper. The implantation was carried out at 17 different energies, in a sequence starting at 450 keV and going down to 50 keV in steps of 25 keV. The dose implanted at each energy was adjusted to yield a nearly uniform C concentration of $1\times 10^{20}\,cm^{-3}$ in the range from 0.1 to 1.0 μm below the surface of the sample. A few samples were coimplanted with $^{12}C^+$ and $^{13}C^+$ into overlapping profiles with $1\times 10^{20}\,cm^{-3}$ of each isotope. The implantation was carried out at room temperature and at a background pressure of 5×10^{-7} torr. The normal of the $8\times 8\,mm^2$ surfaces was tilted 7° off the direction of the C^+ beam to reduce channeling effects during implantation. Furthermore, the beam was swept horizontally and vertically across the sample to ensure a homogeneous lateral distribution of implants. The sample holder was electrically insulated from the vacuum chamber, and the implanted dose was determined directly from integration of the current to the sample. Emission of secondary electrons was suppressed by a negative potential supplied to a shield surrounding the sample.

The infrared absorption spectrum of each sample was recorded after each step in a series of isochronal heat treatments (annealings). Each annealing was performed in a furnace continuously flowed with nitrogengas. The duration of each annealing was 20 min and during this time the temperature was stable to within ± 2 °C. The first annealing was carried out at 300 °C, and in each subsequent step the temperature was increased by 50 °C. Prior to each annealing and before each measurement, all samples were etched in 1% hydroflouricacid to remove surface oxides.

The infrared absorbance spectra were recorded with a Nicolet, System 800, Fourier-transform spectrometer, equipped with a closed cycle helium cryostat with CsI windows. The measurements were carried out at 9 K with an apodized resolution of 3.4 cm^{-1} in the spectral range from 400 to 4000 cm^{-1}. We used a Ge-KBr beamsplitter, a globar light source, and a Mercury-Cadmium-Telluride detector. Absorbance spectra measured on nonimplanted $Si_{1-x}Ge_x$ samples were subtracted from all spectra recorded on the implanted samples.

III. VIBRATIONAL PROPERTIES OF C_s IN $Si_{1-x}Ge_x$

A. Frequencies of local modes

In order to guide the assignment of the observed local vibrational modes to C_s, we now discuss the expected vibrational properties of this defect in $Si_{1-x}Ge_x$. Because we are interested only in local modes, the C_s defect is described as a five atom molecule, with a central C atom and four tetrahedrally coordinated Si and Ge atoms, labeled Y_1, Y_2, Y_3, and Y_4 in Fig. 1. It is assumed that the positions of the four neighbor atoms do not depend on the detailed distribution of Si and Ge atoms in the surrounding lattice. However, we expect that the many different configurations of the surrounding lattice show up as a broadening of the absorption lines associated with the local vibrational modes of C_s.

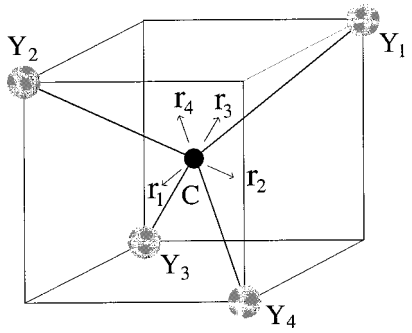

FIG. 1. Molecular model of C_s bound to four lattice atoms Y_i, where Y_i is Si or Ge. The displacement coordinates r_i associated with stretching of the Y_i-C bonds are sketched.

The bend modes of the five-atom molecule involve mainly Si and Ge atoms. Consequently, these modes will have low frequencies and be delocalized due to strong coupling with the lattice phonons. The stretching modes will have higher frequencies and be approximately decoupled from the other modes. We assume that the valence-force approximation[16] is valid and express the potential energy term for the stretch mode vibrations as

$$V = 1/2\sum_{i=1}^{4} f_{Y_i} r_i^2, \tag{1}$$

where r_i is the extension coordinate of the Y_i-C bond indicated in Fig. 1 and f_{Yi} is the effective force constant of the Y_i-C bond. There are five different configurations of nearest neighbors, which we denote $Si_{4-n}Ge_n$:C $(0\leqslant n\leqslant 4)$. For a given configuration, the $4-n$ Si-C bonds are equivalent and the same applies for the n Ge-C bonds. Therefore, only two force constants f_s (Si-C bonds) and f_g (Ge-C bonds) are needed for a given configuration. With standard techniques[16] the frequencies of $Si_{4-n}Ge_n$:C can be calculated and expressed as functions of f_s, f_g, and the atomic masses. The results are summarized in Table I. As can be seen from the table, the five configurations give rise to a total of nine C modes. The number of modes for each configuration is easily found from group theory Si_4Ge_0:C and Si_0Ge_4:C have T_d-point group and possess a single three-dimensional C mode, denoted T_2 in accordance with the irreducible representation describing its symmetry properties. The configurations with C_{3v} symmetry, Si_3Ge_1:C and Si_1Ge_3:C, have a two-dimensional E mode and a nondegenerate A_1 mode. Finally, Si_2Ge_2:C has C_{2v} symmetry, which results in three nondegenerate modes, denoted B_1, B_2, and A_1.

At a first glance, some of the frequencies in Table I appear identical. However, f_s and f_g depend on the length of the Si-C and Ge-C bonds, which depend on the configuration as well as the composition x of the $Si_{1-x}Ge_x$ sample. In the

TABLE I. The square of the local mode frequencies of C_s for all configurations of $Si_{4-n}Ge_n$:C.

Config.	Mode	ω^2
Si_4Ge_0:C	T_2	$\left(\frac{4}{3m_c}+\frac{1}{m_s}\right)f_s$
Si_3Ge_1:C	A_1	$\frac{1}{2}\left\{\left(\frac{1}{3m_c}+\frac{1}{m_s}\right)f_s+\left(\frac{1}{m_c}+\frac{1}{m_g}\right)f_g + \sqrt{\left[\left(\frac{1}{3m_c}+\frac{1}{m_s}\right)f_s-\left(\frac{1}{m_c}+\frac{1}{m_g}\right)f_g\right]^2+\frac{4}{3m_c^2}f_sf_g}\right\}$
	E	$\left(\frac{4}{3m_c}+\frac{1}{m_s}\right)f_s$
Si_2Ge_2:C	A_1	$\frac{1}{2}\left\{\left(\frac{2}{3m_c}+\frac{1}{m_s}\right)f_s+\left(\frac{2}{3m_c}+\frac{1}{m_g}\right)f_g + \sqrt{\left[\left(\frac{2}{3m_c}+\frac{1}{m_s}\right)f_s-\left(\frac{2}{3m_c}+\frac{1}{m_g}\right)f_g\right]^2+\frac{16}{9m_c^2}f_sf_g}\right\}$
	B_1	$\left(\frac{4}{3m_c}+\frac{1}{m_s}\right)f_s$
	B_2	$\left(\frac{4}{3m_c}+\frac{1}{m_g}\right)f_g$
Si_1Ge_3:C	A_1	$\frac{1}{2}\left\{\left(\frac{1}{3m_c}+\frac{1}{m_g}\right)f_g+\left(\frac{1}{m_c}+\frac{1}{m_s}\right)f_s + \sqrt{\left[\left(\frac{1}{3m_c}+\frac{1}{m_g}\right)f_g-\left(\frac{1}{m_c}+\frac{1}{m_s}\right)f_s\right]^2+\frac{4}{3m_c^2}f_sf_g}\right\}$
	E	$\left(\frac{4}{3m_c}+\frac{1}{m_g}\right)f_g$
Si_0Ge_4:C	T_2	$\left(\frac{4}{3m_c}+\frac{1}{m_g}\right)f_g$

appendix, it is described how the values of f_s and f_g may be estimated. For the configuration $Si_{4-n}Ge_n$:C the result is

$$f_s = f_s^0\left[1-\frac{2\alpha\Delta b}{R^0_{\text{Si-C}}}\frac{f_g^0(4x-n)}{(4-n)f_g^0+nf_s^0}\right] \tag{2}$$

$$f_g = f_g^0\left[1-\frac{2\alpha\Delta b}{R^0_{\text{Ge-C}}}\frac{f_s^0(4x-n)}{(4-n)f_g^0+nf_s^0}\right] \tag{3}$$

where $f_s^0 = 9.235\,\text{eV Å}^{-2}$ is the value of f_s for Si_4Ge_0:C in pure Si and $R^0_{\text{Si-C}} = 1.962$ Å is the corresponding bondlength (see Sec. V). Likewise, $f_g^0 = 8.302\,\text{eV Å}^{-2}$ is the value of f_g for Si_0Ge_4:C in pure Ge and $R^0_{\text{Ge-C}} = 2.035$ Å is the corresponding bondlength. Finally, $\alpha\Delta b$ is a factor with dimension of length. The value of $\alpha\Delta b$ has been adjusted to obtain frequency variations with x in reasonable agreement with the observations described below. The best agreement is obtained with $\alpha\Delta b = 0.16$ Å, and this value is used throughout. With the expression given in Table I and Eqs. (2)–(3), the frequencies for all configurations $Si_{4-n}Ge_n$:C can be estimated at any value of x.

At this point we mention that Kulik *et al.*[13] resently calculated local mode frequencies of $Si_{4-n}Ge_n$:C in $Si_{1-x}Ge_x$, using an anharmonic Keating model. The results obtained by these authors qualitatively agree with our findings.

B. Intensities of local modes

To estimate the population of each configuration $Si_{4-n}Ge_n$:C from the observed spectra, we need to elaborate further on the model described above. We assume that the dipole moment induced by the stretching of a bond is parallel to the bond and that the total dipole moment of C_s can be calculated as the sum of the dipole moments of the four bonds. To first order in the displacement coordinates $r_i (i = 1,2,3,4)$, the dipole moment $\mathbf{d}$ is then given by

$$\mathbf{d} = \mathbf{d}_0 + \sum_{i=1}^{4} e_i r_i \hat{\mathbf{n}}_i, \tag{4}$$

where $\mathbf{d}_0$ is the permanent dipole moment, e_i is the derivative of the dipole moment with respect to r_i, which we denote the effective charge of the Y-C bond, and $\hat{\mathbf{n}}_i$ is a unit vector pointing from the ith neighbor atom Y_i towards C (see Fig. 1). For a given configuration the effective charge $e_s(n)$ [or $e_g(n)$] is the same for all Si-C (or Ge-C) bonds since they are equivalent. The integrated absorption coefficient (in-

tensity) of the local mode Γ associated with the configuration $Si_{4-n}Ge_n$:C may be expressed as[16]

$$I_\Gamma(n)=\frac{2\pi^2 N_{\rm tot}}{3n_R c}p(n)\mu_\Gamma(n)^2. \tag{5}$$

$N_{\rm tot}$ is the total concentration of C_s, $p(n)$ is the fraction of complexes with configuration $Si_{4-n}Ge_n$, n_R is the refractive index, and c is the velocity of light. The parameter $\mu_\Gamma(n)$ is given by

$$\mu_\Gamma(n)^2=\sum_{a=1}^{m_\Gamma}\left(\frac{\partial \mathbf{d}}{\partial Q_{\Gamma a}}\right)^2, \tag{6}$$

where $\{Q_{\Gamma a}\}$ is the set of normal coordinates associated with the normal mode Γ, and m_Γ is the dimension of the mode. The parameter $\mu_\Gamma(n)$ is a function (quadratic form) of the effective charges $e_s(n)$ and $e_g(n)$, which are unknown. In addition, $N_{\rm tot}$ is not known in our samples. Hence, we cannot obtain $p(n)$ by inserting the measured value of $I_\Gamma(n)$ into Eqs. (5)–(6). However, for a given composition x, the value of $p(n)e_s(n)^2$ normalized to $p(0)e_s(0)^2$ can for $n \in\{0,1,2,3\}$ be determined from the formula

$$[p(n)e_s(n)^2]_{\rm rel}\equiv\frac{p(n)e_s(n)^2}{p(0)e_s(0)^2}=\frac{I_\Gamma(n)}{I_{T_2}(0)}\left[\frac{\mu_{T_2}(0)e_s(n)}{e_s(0)\mu_\Gamma(n)}\right]^2. \tag{7}$$

For $n\in\{1,2,3\}$ the value of $\mu_\Gamma(n)/e_s(n)$ depends for some modes on the ratio $e_g(n)/e_s(n)$, which can be obtained from the intensity ratio between two different modes of the same configuration $Si_{4-n}Ge_n$:C.

As discussed above, the Si-C and Ge-C bondlengths vary with changes in x and from one configuration to another. Because the first derivative of the bond-dipole moment may depend on the length of the bond, $e_s(n)$ and $e_g(n)$ may depend on x as well as on the specific configuration of the neighboring atoms. However, for a given composition x, the bondlengths differ by less than 5% between the different configurations. Thus, we suspect that $e_s(n)$ does not change dramatically with n at a given x.

Therefore, we expect that $[p(n)e_s(n)^2]_{\rm rel}$ approximately equals the relative population, $[p(n)]_{\rm rel}\equiv p(n)/p(0)$, of $Si_{4-n}Ge_n$:C. If the distribution of the four Si and Ge neighbors is random, $[p(n)]_{\rm rel}$ is easily calculated for all compositions

$$[p(n)]_{\rm rel}=\binom{4}{n}\left(\frac{x}{1-x}\right)^n. \tag{8}$$

IV. EXPERIMENTAL RESULTS

A. Observation of local vibrational modes of C_s

Two broad absorption bands at ~542 and ~584 cm^{-1} are observed in $Si_{0.50}Ge_{0.50}$ after implantation of $^{12}C^+$ and subsequent annealing at 550 °C, as can be seen from curve *a* in Fig. 2. A similar pair of bands is observed when $^{12}C^+$ is substituted by $^{13}C^+$ (see curve *b*) but the frequencies are shifted downwards by a factor of ~1.03, which is close to 13/12. Therefore, the bands represent local vibrational modes of C bound to a heavier element.

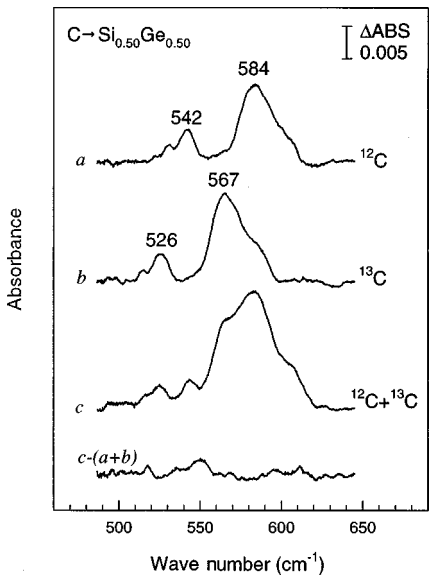

FIG. 2. Absorbance spectra measured at 9 K on $Si_{0.50}Ge_{0.50}$ samples annealed at 550 °C after implantation with (a) $^{12}C^+$, (b) $^{13}C^+$, and (c) equal doses of both isotopes. The spectrum at the bottom is the result of subtracting spectra of the isotopic pure samples (curves a and b) from the spectrum of the coimplanted sample (curve c).

Coimplantation of $^{12}C^+$ and $^{13}C^+$ produces a spectrum with an even broader absorption band, depicted as curve *c* in the figure. When the coimplanted spectrum is subtracted by the single isotope spectra, the resulting spectrum is basically flat (see Fig. 2). Hence, the bands at about 542 and 584 cm^{-1} originate from defects, which contain a single C atom. Similar bands have been observed for all compositions x and in all cases they are found to represent local modes of defects, which contain a single C atom.

The absorbance spectra recorded after annealing at 550 °C on $^{13}C^+$-implanted $Si_{1-x}Ge_x$ samples with different compositions are shown in Fig. 3. Each spectrum is depicted so that its base line corresponds to the composition of the sample. For pure Si, a single absorption line reflecting the T_2 mode of $^{13}C_s$ is observed at 589 cm^{-1} (Ref. 10). Likewise, a single line at 512 cm^{-1} observed in pure Ge represents the T_2 mode of $^{13}C_s$ in that material.[11] As the Ge content is increased from $x=0$, the T_2 line broadens into a band of lines and shifts downwards in frequency. When the Ge content exceeds ~15 at. % another broad band appears at lower frequencies, which also shifts downwards in frequency with increasing Ge content. As can be seen from the figure, the two bands are for all configurations largely confined to the frequency interval defined by the T_2 lines of the pure materials. Moreover, the frequency shifts with composition x indicate that in the limits $x\rightarrow 0$ and $x\rightarrow 1$, the high- and low-frequency bands transform into the T_2 lines of pure Si and Ge, respectively. This strongly suggests that the bands originate from different configurations of C_s. This assignment is consistent with the involvement of a single C atom in each of the underlying defects.

The frequencies calculated for all configurations of $^{13}C_s$ from the formulas in Sec. III are also depicted in Fig. 3 as straight lines. A line is shown solid in the composition range, where the intensity of the corresponding mode is expected to

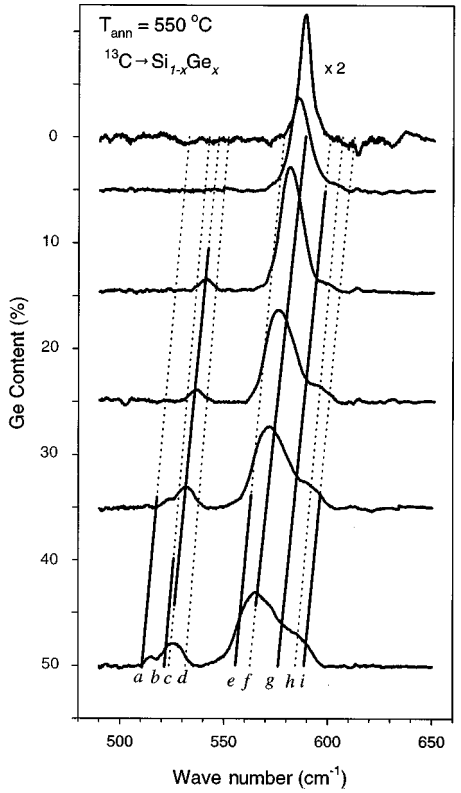

FIG. 3. Absorbance spectra recorded at 9 K on $^{13}C^+$-implanted $Si_{1-x}Ge_x$ samples with different compositions ($0 \leqslant x \leqslant 1$) after annealing at 550 °C. The baseline of each spectrum is displaced vertically to correspond to the composition of the corresponding sample. The straight lines are calculated from the model described Sec. III A. Each line shows the variation in frequency for one specific mode as a function of Ge concentration. A line is shown solid in the composition range, where the intensity of the corresponding mode is expected to exceed 10% of the total intensity of all C_s modes, and the dotted part of the lines corresponds to the range where the modes are expected to be very weak. The labels correspond to individual modes: (a) B_2 mode of Si_2Ge_2:C, (b) E mode of Si_1Ge_3:C, (c) A_1 mode of Si_3Ge_1:C, (d) T_2 mode of Si_0Ge_4:C, (e) A_1 mode of Si_2Ge_2:C, (f) T_2 mode of Si_4Ge_0:C, (g) E mode of Si_3Ge_1:C, (h) A_1 mode of Si_1Ge_3:C, and (i) B_1 mode of Si_2Ge_2:C.

exceed 10% of the total intensity of all C_s modes. The dotted part of the lines indicates the composition range where the modes are expected to be very weak. To estimate the composition ranges, it has been assumed that the distribution of the four neighbors to the C is random.

The spectra recorded on the ^{13}C-implanted $Si_{0.65}Ge_{0.35}$ sample after annealing at 550 and 750 °C are shown in Fig. 4. Four lines denoted L_1, L_2, L_4+L_5, and L_6 are resolved. According to Fig. 3, the modes of the configurations Si_4Ge_0:C, Si_3Ge_1:C, and Si_2Ge_2:C are expected to dominate the spectrum for this composition $x=0.35$. Based on the close similarity with the model frequencies, we ascribe the L_1 line to the B_2 mode of Si_2Ge_2:C and the L_2 line to the A_1 mode of Si_3Ge_1:C. The intensity of the L_6 line increases somewhat when the annealing temperature is increased from 550 to 750 °C. A similar behavior is observed for the L_1 line, whereas the L_2 line is constant. Therefore, we ascribe the L_6 line to the B_1 mode of Si_2Ge_2:C. The E mode of Si_3Ge_1:C and the T_2 mode of Si_4Ge_0:C should correspond to the two

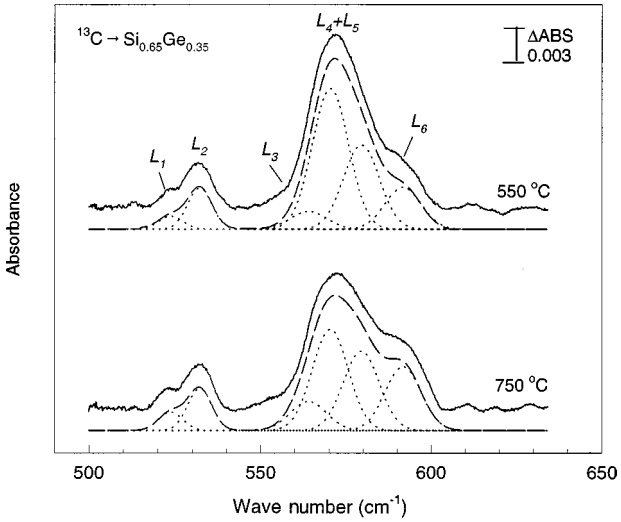

FIG. 4. Spectra recorded at 9 K on a ^{13}C-implanted $Si_{0.65}Ge_{0.35}$ sample annealed at 550 and 750 °C. The individual lines are denoted L_1, L_2, L_3, L_4, L_5, and L_6. The best overall fit to the spectra and the individual components are shown as dashed and dotted curves.

most prominent lines in the spectrum, according to our intensity estimates. This strongly suggests that the line L_4+L_5 consists of two overlapping lines L_4 and L_5, which represent the T_2 mode of Si_4Ge_0:C (L_4 line) and the E mode of Si_3Ge_1:C (L_5 line). Additional evidence for this is provided by the spectrum recorded after annealing at 750 °C. In this case, the line profile of L_4+L_5 is clearly asymmetric. The low-frequency tail of the line L_4+L_5 is rather broad, which indicates the presence of yet a line, labeled L_3. From comparison with Fig. 3, we ascribe this line to the A_1 mode of Si_2Ge_2:C. Hence, the existence of the L_3 line is consistent with the assignment of the L_1 and L_6 lines to the B_2 and B_1 modes of the same complex.

The spectra in Fig. 4 have been fitted with a sum of six Gaussians[17] corresponding to the lines L_1, L_2, L_3, L_4, L_5, and L_6. The best fit and the individual components are also shown in the figure, and the peak positions and intensities are presented in Table II. The widths of the gaussians corresponding to L_3, L_4, L_5, and L_6 were forced to be equal during the fit, as were the widths of the Gaussians representing L_1 and L_2.

A similar procedure has been applied to fit the observed spectra for all compositions covered in this study. The best-fit parameters are also given in Table II together with the assignment of the individual components.

B. Analysis of local mode intensities

On basis of the local mode intensities given in Table II, $[p(n)e_S(n)^2]_{rel}$ can be calculated for $x=0.15,0.25,0.35,0.50$. As mentioned in Sec. III, we expect that $[p(n)e_S(n)^2]_{rel}$ approximately equals the relative population distribution $[p(n)]_{rel}$ of the four Si and Ge neighbors. In Table III, the values obtained for $[p(n)e_S(n)^2]_{rel}$ are compared with those of $[p(n)]_{rel}$ corresponding to a random distribution of neighbors [see Eq. (8)]. When x is small, the random-distribution values of $[p(n)]_{rel}$ agree with the values of $[p(n)e_S(n)^2]_{rel}$. However, when x exceeds 0.25, the two

TABLE II. Peak positons ω (cm^{-1}) and intensities I (cm^{-1}) of the individual modes determined from the best fit to the spectra recorded on $Si_{1-x}Ge_x$ after implantation of ^{13}C and subsequent annealing at 550 °C. The frequencies and the intensities marked with an * are uncertain, as these absorption lines may mix with lines from the configuration Si_1Ge_3:C.

Configuration and mode	x	0.00	0.05	0.15	0.25	0.35	0.50
Si_4Ge_0:C							
T_2 mode	ω	589.0	586.5	580.6	575.4	570.4	563.0
(L_4 line)	I	0.075	0.194	0.209	0.195	0.166	0.144
Si_3Ge_1:C							
A_1 mode	ω			541.4	536.6	532.2	525.7*
(L_2 line)	I			0.017	0.018	0.032	0.043*
E mode	ω			586.6	583.9	579.5	573.2
(L_5 line)	I			0.097	0.082	0.099	0.114
Si_2Ge_2:C							
B_2 mode	ω					523.8	515.5
(L_l line)	I					0.011	0.014
A_1 mode	ω			571.0	569.0	564.0	556.0
(L_3 line)	I			0.008	0.019	0.021	0.031
B_1 mode	ω			600.0	596.1	591.8	585.4*
(L_6 line)	I			0.013	0.030	0.050	0.086*

sets of values deviate significantly, which indicates a nonrandom distribution of nearest neighbors. Instead, the values of $[p(n)e_S(n)^2]_{rel}$ suggest a substantial preference for formation of complexes with many (3 or 4) Si neighbors.

Next, we discuss the thermal stability of the individual modes. Absorption spectra recorded on ^{13}C-implanted $Si_{0.65}Ge_{0.35}$ after annealing at different temperatures have been fitted with a sum of six Gaussians, with peak positions and widths fixed at the values obtained from the spectrum recorded after annealing at 550 °C, as described in Sec. IV A. The resulting intensities of the individual components are shown against annealing temperature in Fig. 5. All modes appear at about 525 °C and anneal at about 875 °C. The detailed annealing behaviors of the modes differ, but modes assigned to the same configuration display the same behavior. This provides additional support for the assignments made above. The intensity of the T_2 mode of Si_4Ge_0:C reaches maximum at ~550 °C and decreases gradually as the annealing temperature is increased further up to 850 °C. In contrast, the A_1 and E modes of Si_3Ge_1:C have nearly constant intensities from 550 °C up to 850 °C, and the modes of Si_2Ge_2:C display a gradual intensity increase in this temperature range. Hence, the relative populations of the different configurations change from 550 to 850 °C. From the intensities obtained after annealing at 850 °C, we find that $[p(0)e_s(0)^2]_{rel}=1.0$, $[p(1)e_s(1)^2]_{rel}=1.1$, and $[p(2)e_s(2)^2]_{rel}=1.0$. Comparison with the (550 °C) values in Table II suggests that after 850 °C annealing the distribution of neighbor atoms is closer to, but remains significantly different from, a random distribution. We note that the thermodynamical equilibrium distribution will differ from a random distribution, unless the total energies of all configura-

TABLE III. Calculated values of $[p(n)e_s(n)^2]_{rel}$, and the random-distribution values of $[p(n)]_{rel}$ as a function of Ge content x. All intensities were determined from spectra measured after annealing at 550 °C.

x	0.15	0.25	0.35	0.50
Model				
$[p(0)e_s(0)^2]_{rel}$	1.00	1.00	1.00	1.00
$[p(1)e_s(1)^2]_{rel}$	0.70	0.64	0.90	1.20
$[p(2)e_s(2)^2]_{rel}$	0.18	0.45	0.58	1.04
$[p(3)e_s(3)^2]_{rel}$				
Random				
$[p(0)]_{rel}$	1.00	1.00	1.00	1.00
$[p(1)]_{rel}$	0.71	1.33	2.15	4.00
$[p(2)]_{rel}$	0.19	0.67	1.74	6.00
$[p(3)]_{rel}$	0.02	0.15	0.62	4.00
$[p(4)]_{rel}$	0.00	0.01	0.08	1.00

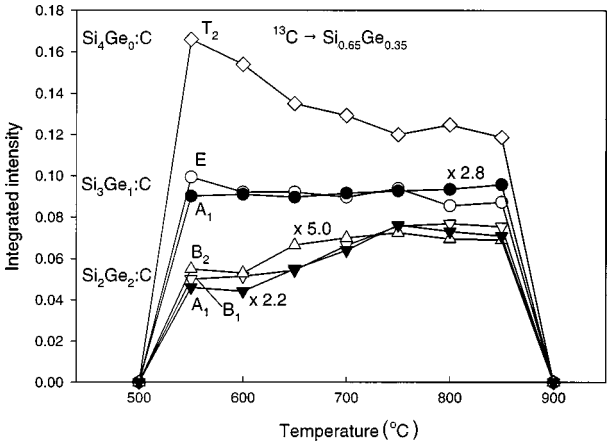

FIG. 5. Intensities of the individual modes of $^{13}C_s$ in $Si_{0.65}Ge_{0.35}$ shown against annealing temperature. The intensity of the A_1 mode of Si_3Ge_1:C has been scaled by a factor of 2.8. The intensities of the A_1 and B_2 modes of Si_2Ge_2:C have been scaled by 2.2 and 5.0, respectively.

tions $Si_{4-n}Ge_n$:C are identical. Thus, deviations from a random distribution may not be surprising.

V. THEORETICAL CALCULATIONS

A. Method

In order to further investigate the credibility of the assignments made in Sec. IV A, the structure and local vibrational modes of $Si_{4-n}Ge_n$:C embedded in a Si and a Ge cluster have been calculated using *ab initio* local density-functional theory.[18] The calculations were made on 71-atom tetrahedral clusters, $Si_{35}H_{36}$ and $Ge_{35}H_{36}$, where the central Si or Ge atom was replaced by a C atom and the dangling bonds on the surface of the cluster were terminated by infinitely massive H atoms. The wave functions were represented by a basis set of Guassian orbitals: Eight Gaussian orbitals of different exponents were centered on the C atom and four orbitals on the inner four Si and Ge neighbor atoms. A fixed linear combination of four orbitals was used for the remaining Si or Ge atoms, and a fixed linear combination of three orbitals was placed on each of the H atoms on the surface. Finally, three *s*- and *p*-Gaussian orbitals were placed at the center of every Si-Si or Ge-Ge bond in the cluster. The self-consistent energy and the forces on the atoms were calculated, and all 34 host atoms together with the C atom were allowed to relax until the minimum-energy configuration was obtained. During this calculation, full symmetry constraints were applied, and the H atoms at the surface were fixed at their starting positions. To calculate the local vibrational modes of the defect, the second derivatives of the energy with respect to atomic positions were calculated directly for the C atom and its four neighbors while the derivatives for the remaining atoms were calculated from a Musgrave-Pople potential.[19,20]

The C_s atom was first placed at the center of the Si cluster and the optimized positions and local vibrational modes were found. The four Si neighbors of the C atom were then replaced one at a time by Ge atoms, the structure was reoptimized, and the new local modes of the $Si_{4-n}Ge_n$:C configurations in a bulk Si cluster were calculated. The above process was then carried out in a Ge cluster with the nearest neighbors to C being replaced in turn by Si atoms to obtain the modes in bulk Ge.

B. Results

The optimized bondlengths of $Si_{4-n}Ge_n$:C are given in Table IV and the calculated modes are given in Table V for the ^{12}C and ^{13}C isotopes. We note that the Si-C bondlength of Si_4Ge_0:C in pure Si is 1.962 Å in good agreement with x-ray studies on C-doped Si, which gave a value of 1.95 Å.[21]

As can be seen from Table IV, the Si-C and Ge-C bondlengths decrease as the number of Ge neighbors are increased in both materials. The reason is that the Si-C bonds have a larger force constant than the Ge-C bonds. Hence, the C atom is displaced from its lattice site in a direction, which causes the Si-C bonds to shorten and the Ge-C bonds to lengthen compared to the ideal ''unrelaxed'' structures. Due to the near-tetrehedral coordination of the four neighbors, this effect is larger the more Ge neighbors there are.

TABLE IV. Calculated Si-C and Ge-C bondlengths (Å) of C_s in Si and Ge clusters for all configurations of nearest neighbors $Si_{4-n}Ge_nC$.

Configuration	Point group	Si-C	Ge-C
Si cluster			
Si_4Ge_0:C	T_d	1.962	
Si_3Ge_1:C	C_{3v}	1.954	2.043
Si_2Ge_2:C	C_{2v}	1.947	2.033
Si_1Ge_3:C	C_{3v}	1.938	2.027
Si_0Ge_4:C	T_d		2.018
Ge cluster			
Si_4Ge_0:C	T_d	1.977	
Si_3Ge_1:C	C_{3v}	1.966	2.065
Si_2Ge_2:C	C_{2v}	1.957	2.053
Si_1Ge_3:C	C_{3v}	1.951	2.044
Si_0Ge_4:C	T_d		2.035

If we take the trigonal (C_{3v}) defect Si_3Ge_1:C in the Si matrix as an example: The Si-C bond length is 0.008 Å shorter than that of Si_4Ge_0:C and the Ge-C bondlength is 0.025 Å longer than that of Si_0Ge_4:C. Due to the short Si-C bonds, the *E* mode of Si_3Ge_1:C has higher frequency than the T_2 mode of Si_4Ge_0:C. This is in violation of the Saxon Hutner theorem.[22] However, this theorem assumes that the force constants are identical so that the shifts in the frequencies are entirely due to the difference in the masses of the constituents. Clearly, this assumption is not fulfilled in the present case since the force constants largely reflect the bond lengths.

The first-principle frequencies are often overestimated and to bring them in closer agreement with experiment we scale the theoretical values by the factor 0.917. This gives the T_2 modes for ^{13}C at 589 cm^{-1} in Si (Ref. 10) and at 512 cm^{-1} in Ge (Ref. 11) in perfect agreement with the observed modes. That the same scaling factor is required for both Si and Ge suggests that this factor is appropriate for all the modes of $Si_{4-n}Ge_n$:C in the alloy.

It is clear that for low *x*, the matrix is closer to Si than Ge, whereas it is the reverse for large *x*. Thus, the effect of in-

TABLE V. Calculated frequencies (cm^{-1}) of local vabrational modes for $^{12}C_s$ amd $^{13}C_s$ in Si and Ge clusters for all configurations of nearest neighbors $Si_{4-n}Ge_n$:C. Furthermore, the scaled $^{13}C_s$ mode frequencies of $Si_{0.65}Ge_{0.35}$ are given.

		^{12}C		^{13}C		$x=0.35$
Configuration	Mode	Si	Ge	Si	Ge	
Si_4Ge_0:C	T_2	662	638	642	618	580
Si_3Ge_1:C	A_1	612	588	593	569	536
	E	673	651	653	631	592
Si_2Ge_2:C	B_2	594	568	574	548	518
	A_1	642	617	623	598	563
	B_1	684	663	664	642	602
Si_1Ge_3:C	E	598	573	578	552	522
	A_1	675	649	655	629	592
Si_0Ge_4:C	T_2	605	579	583	558	526

creasing x is to cause an expansion of the Si-C and Ge-C bonds as can be inferred from Table IV. This expansion causes a drop in each frequency and we assume that the frequencies of $Si_{4-n}Ge_n$:C in the alloy can be obtained from linear interpolation of the corresponding scaled frequencies in the Si and Ge matrices. The frequencies thus obtained for $^{13}C_s$ in an alloy with $x=0.35$ are also given in Table V. As can be seen from comparison with Table II, there is a close correspondence between the calculated and assigned frequencies for the $Si_{4-n}Ge_n$:C defects ($n=0$, 1, and 2). The numerical ordering of the individual modes agrees and the maximum deviation between the two sets of frequencies is only 12 cm^{-1}. Hence, we conclude that the *ab initio* calculations provide additional support for the assignments made in Sec. IV A.

The calculations show that there is an energy preference for C to form bonds with Si rather than Ge. By comparing the energies of two relaxed clusters $CGeSi_{69}H_{60}$, where the Ge atom is a nearest or second-nearest neighbor to C, the Si-C bond was favored by 0.2 eV. Similarly, in the clusters $CSiGe_{69}H_{60}$, the C-Si bond was favored by 0.25 eV. These values suggest that the equilibrium probability of C being surrounded by four Ge neighbors in the alloy is negligible even at 850 °C. Thus, the deviation from a random distribution of neighbors discussed in Sec. IV B is in accordance with the *ab initio* results.

VI. CONCLUSION

Infrared absorption spectroscopy has been applied to study C_s in ^{13}C-implanted $Si_{1-x}Ge_x$ as a function of composition x. It has been shown that C_s possesses local vibrational modes with frequencies in the range from 512 to 600 cm^{-1}. The frequencies were calculated from a harmonic model, and the results are used to assign the observed absorption bands. According to our assignments, C_s binds to both Si and Ge neighbor atoms. The intensities of the local modes strongly suggest that the distribution of the four neighbor atoms is not random, but there is a preference for the configuration with four Si neighbors. *Ab initio* local density functional cluster theory has been used to calculate the structure of $Si_{4-n}Ge_n$:C and the frequencies of the associated local modes. The results are in good agreement with our observations and provide additional support for our assignments.

ACKNOWLEDGMENTS

This work has been supported by the Danish National Research Foundation through Aarhus Center for Advanced Physics (ACAP) J. L. Hansen and P. Bomholt are gratefully acknowledged for growing and preparing the $Si_{1-x}Ge_x$ samples. R.J. and A.N.L. thank the ENDEASD Network for support. S.Ö. thanks NFR and TFR in Sweden for financial support and also PDC at KTH for computer time on the SP2.

APPENDIX

As mentioned in Sec. III the effective force constants f_s and f_g depend on the length of the Si-C and Ge-C bonds. For a diatomic molecule *Y-Z* with bondlength $R_{Y\text{-}Z}$ and stretch frequency $\omega_{Y\text{-}Z}$, Morse[23] proposed the empirical relation

$$\omega_{Y-Z}R_{Y-Z}^{\alpha}=\text{Constant}, \tag{A1}$$

where $\alpha\sim 3$ as a rough estimate. We assume that this relation also holds for the Y_i-C bonds of the molecules in Fig. 1. Equation (A1) implies that for small changes in the bondlength the effective force constant f_Y for a *Y-C* bond is given by

$$f_Y=f_Y^0\left(1-2\alpha\frac{dR_{Y-C}}{R_{Y-C}^0}\right), \tag{A2}$$

where R_Y^0 and f_Y^0 are the bond length and the effective force constant for a reference state. Moreover, $dR_{Y\text{-}C}=R_{Y\text{-}C}-R_{Y\text{-}C}^0$. As a reference state, we choose Si_4Ge_0:C in pure Si for Si-C bonds and Si_0Ge_4:C in pure Ge for Ge-C bonds. From the frequencies of the T_2 modes, 607 cm^{-1} in Si (Ref. 10) and 531 cm^{-1} in Ge,[11] and with the expressions in Table I, we calculate $f_s^0=9.235\,\text{eV Å}^{-2}$ and $f_g^0=8.302\,\text{eV Å}^{-2}$. Since reasonable estimates of $R_{\text{Si-C}}^0$ and $R_{\text{Ge-C}}^0$ are sufficient we use the theoretical values, $R_{\text{Si-C}}^0=1.962$ Å and $R_{\text{Ge-C}}^0=2.035$ Å, given in Sec. V.

Now we denote the Si-C bondlength for Si_4Ge_0:C by $b_s(x)$ and the Ge-C bondlength for Si_0Ge_4:C by $b_g(x)$. With this definition, $b_s(0)=R_{\text{Si-C}}^0$ and $b_g(1)=R_{\text{Ge-C}}^0$. Since the variations of $b_s(x)$ and $b_g(x)$ as x is changed are less than a few percent, we expect that linear expansions are valid

$$b_s(x)=R_{\text{Si-C}}^0+x\Delta b_s$$

$$0\leqslant x\leqslant 1$$

$$b_g(x)=R_{\text{Ge-C}}^0+(1-x)\Delta b_g \tag{A3}$$

where $\Delta b_Y=b_Y(1)-b_Y(0)$. The values of Δb_s and Δb_g are unknown. According to the *ab initio* calculations described in Sec. V, Δb_s and Δb_g differ only by 0.02 Å. Therefore, we set $\Delta b\equiv\Delta b_s=\Delta b_g$.

To estimate $R_{\text{Si-C}}(x)$ and $R_{\text{Ge-C}}(x)$ for the configuration $Si_{4-n}Ge_n$:C, the $4-n$ Si and n Ge atoms are fixed at sites displaced along ⟨111⟩ directions from the origo (see Fig. 1). The distance from each neighbor atom to the origo is chosen equal to $b_s(x)$ for the $4-n$ Si and $b_g(x)$ for the n Ge neighbors. Thus, if the C atom is placed at the origo, the bondlengths are identical to those of Si_4Ge_0:C and Si_0Ge_4:C. However, for complexes with both Si and Ge neighbors, the origo is not the equilibrium site for C, because f_s and f_g differ. It is a simple task to find the equilibrium site of C, and thus, get the values of $dR_{\text{Si-C}}$ and $dR_{\text{Ge-C}}$ for the configuration $Si_{4-n}Ge_n$:C. Then, the force constants f_s and f_g can be obtained from Eq. (A2) and the result is

$$f_s=f_s^0\left[1-\frac{2\alpha\Delta b}{R_{\text{Si-C}}^0}\frac{f_g^0(4x-n)}{(4-n)f_g^0+nf_s^0}\right]$$

$$f_g=f_g^0\left(1-\frac{2\alpha\Delta b}{R_{\text{Ge-C}}^0}\frac{f_s^0(4x-n)}{(4-n)f_g^0+nf_s^0}\right). \tag{A4}$$

The factor $\alpha\Delta b$ is not known, and as described in Sec. III, its value has been adjusted to reproduce the observed variations of the frequencies with x. The best value was found to be $\alpha\Delta b=0.16$ Å.

[1] For a review see, e.g., *GeSi Strained Layers and Their Applications*, edited by A. M. Stoneham and S. C. Jain (Institute of Physics, Bristol, 1995).
[2] D. C. Houghton, J. Appl. Phys. **70**, 2136 (1991).
[3] K. Eberl, S. S. Iyer, S. Zollner, J. C. Tsang, and F. K. LeGoues, Appl. Phys. Lett. **60**, 3033 (1992).
[4] A. R. Powell and S. S. Iyer, Jpn. J. Appl. Phys., Part 1 **33**, 2388 (1994).
[5] B. Dietrich, H. J. Osten, H. Rücker, M. Methfessel, and P. Zaumseil, Phys. Rev. B **49**, 17 185 (1994).
[6] N. Herbots, P. Ye, H. Jacobsson, J. Xiang, S. Hearne, and N. Cave, Appl. Phys. Lett. **68**, 782 (1996).
[7] J. Mi, P. Letourneau, M. Judelewicz, M. Gailhanou, M. Dutoit, C. Dubois, and J. C. Dupuy, Appl. Phys. Lett. **67**, 259 (1995).
[8] J. L. Regolini, S. Bodnar, J. C. Oberlin, F. Ferrieu, M. Gauneau, B. Lambert, and P. Boucaud, J. Vac. Sci. Technol. A **12**, 1015 (1994).
[9] J. W. Strane, H. J. Stein, S. R. Lee, B. L. Doyle, S. T. Picraux, and J. W. Mayer, Appl. Phys. Lett. **63**, 2786 (1993).
[10] R. C. Newman and J. B. Willis, J. Phys. Chem. Solids **26**, 373 (1965).
[11] L. Hoffmann, J. C. Bach, B. Bech Nielsen, P. Leary, R. Jones, and S. Öberg, Phys. Rev. B **55**, 11 167 (1997).
[12] L. Hoffmann, J. C. Bach, J. Lundsgaard Hansen, A. Nylandsted Larsen, B. Bech Nielsen, P. Leary, R. Jones, and S. Öberg, in *Proceedings of the International Conference on Defects in Semiconductors, ICDS-19, 1997*, edited by G. Davies and M. H. Nazaré (Trans Tech, Uetikon-Zuerich, Switzerland, 1997), Pt. 1, p. 91.
[13] L. V. Kulik, C. Guedj, M. W. Dashiell, J. Kolodzey, and A. Hairie, in *Proceedings of the 24th International Conference on the Physics of Semiconductors, ICPS 24, 1998*, edited by D. Gershoni (World Scientific Publishing, Singapore, 1999).
[14] A. Nylandsted Larsen, J. Lundsgaard Hansen, R. Schou Jensen, S. Y. Shiryaev, and P. Riis Østergaard, Phys. Scr. **T54**, 208 (1994).
[15] E. V. Monakhov, S. Y. Shiryaev, A. Nylandsted Larsen, J. Hartung, and G. Davies, Thin Solid Films **294**, 43 (1997).
[16] See, e.g., E. B. Wilson, Jr., J. C. Decius, and P. C. Cross, *Molecular Vibrations* (Dover, New York, 1955).
[17] Alternatively, we could have chosen Lorentz or Voigt profiles. However, Lorentzian profiles do not fit the observed line shape as well as Gaussian profiles. Voigt profiles give fits of the same quality as the Gaussian profiles. Also the intensities determined for the individual lines from Gaussian- and Voigt-profile fits differ by less than 10%. Gaussian profiles were chosen since they are mathematically simpler than Voigt profiles.
[18] R. Jones, Philos. Trans. R. Soc. London, Ser. A **341**, 351 (1992).
[19] M. J. P. Musgrave and J. A. Pople, Proc. R. Soc. London, Ser. A **268**, 474 (1962).
[20] F. Berg Rasmussen, R. Jones, and S. Öberg, Phys. Rev. B **50**, 4378 (1994).
[21] D. Windisch and P. Becker, Philos. Mag. A **58**, 435 (1988).
[22] J. M. Ziman, *Models of Disorder* (Cambridge University Press, Cambridge 1979), p. 302.
[23] P. M. Morse, Phys. Rev. **34**, 57 (1929).